

Flavor symmetry breaking in the Δ sea

J. J. Ethier,¹ W. Melnitchouk,² F. M. Steffens,³ and A. W. Thomas⁴

¹*Nikhef Theory Group, Science Park 105, 1098 XG Amsterdam, The Netherlands*

²*Jefferson Lab, 12000 Jefferson Avenue, Newport News, Virginia 23606, USA*

³*Institut für Strahlen- und Kernphysik, Universität Bonn, Nussallee 14-16, 53115 Bonn, Germany*

⁴*CSSM and ARC Centre of Excellence for Particle Physics at the Terascale,
Department of Physics, University of Adelaide SA 5005, Australia*

(Dated: September 15, 2018)

The discovery of a sizeable asymmetry in the \bar{u} and \bar{d} distributions in the proton was one of the more consequential experimental findings in hadron physics last century. Although widely believed to be related to the fundamental role of chiral symmetry in QCD, a definitive verification of this hypothesis has remained elusive. We propose a novel test of the role of chiral symmetry in generating the sea flavor asymmetry by comparing the $\bar{d}-\bar{u}$ content in the proton with that in the Δ^+ baryon, where a significant enhancement is expected around the opening of the $N\pi$ decay channel. Recent developments in lattice QCD suggest a promising way to test this prediction in the near future.

As a result of considerable theoretical and experimental effort we now know that the sea of quark-antiquark pairs in the nucleon is far more complex than originally envisaged on the basis of simple quark models or perturbative QCD. The first major surprise was the confirmation in the early 1990s of an integrated excess of \bar{d} over \bar{u} antiquarks in the proton [1], leading to a violation of the Gottfried sum rule [2]. Almost a decade earlier, as a by-product of a study of the excess of non-strange over strange sea quarks predicted within the cloudy bag model [3, 4], it had been shown that the application of chiral symmetry to the structure of the nucleon naturally led to a surplus of \bar{d} over \bar{u} [5].

Once the experimental result was announced, a number of calculations confirmed that the pion cloud picture could indeed explain it quantitatively [6–9]. Furthermore, careful study of the nonanalytic behavior of the sea quarks as a function of quark mass established that the pion cloud contribution was an essential feature of spontaneous symmetry breaking in QCD [10–14]. Studies of the sea using Drell-Yan lepton-pair production [15] in $p\bar{p}$ collisions at Fermilab suggested an unexpected change of sign in $\bar{d}-\bar{u}$ at parton momentum fractions x around 0.3 [16], which is difficult to accommodate naturally within a meson cloud framework [17]. While we await the results of the follow-up SeaQuest experiment [18], designed to explore the asymmetry to larger x , it is imperative to obtain independent confirmation of the physical mechanism.

In this Letter we suggest that a comparison of the $\bar{d}-\bar{u}$ asymmetry in the Δ^+ baryon with that in the proton provides an outstanding opportunity for such a confirmation. To understand why, we recall that the dominant meson-baryon component of the proton wave function arises from quantum fluctuation $p \rightarrow n\pi^+$. As the π^+ contains only a valence \bar{d} antiquark, one naturally expects $\bar{d} > \bar{u}$ in the proton. The process $p \rightarrow p\pi^0$, which is suppressed by a factor of two by isospin couplings, produces equal numbers of \bar{d} and \bar{u} and therefore does not

affect the asymmetry. While the process $N \rightarrow \Delta\pi$ acts to reduce the asymmetry, it is suppressed relative to the dominant process $N \rightarrow N\pi$.

For the Δ^+ baryon, the processes $\Delta \rightarrow \Delta\pi$ and $\Delta \rightarrow N\pi$ both favor π^+ production, and hence also produce an excess of \bar{d} over \bar{u} . The key difference, however, is that because the Δ decay to $N\pi$ is favored energetically, it experiences a significant kinematical enhancement as a function of the pion mass, m_π , as it approaches the $\Delta - N$ mass difference and the decay channel opens up.

In parallel developments, recent progress in the calculation of PDFs in lattice QCD suggests a realistic means to check the prediction. In particular, lattice QCD measurement of the spatial correlation function of quarks within a fast moving hadron could be used [19], after Fourier transformation and renormalization, to obtain a quasi-PDF [20–22], which through a further matching procedure [23–25] can directly yield the desired light-cone PDF over the range $x \in (-1, +1)$. Previous attempts to extract antiquark distributions from lattice QCD were impaired by the difficulty of disentangling the q and \bar{q} content using only the first two or three moments from calculations of matrix elements of local twist-two operators [26]. In contrast, in the quasi-PDF approach one can use the crossing symmetry relation, $\bar{q}(x) = -q(-x)$, to extract directly the x dependence of the \bar{q} PDFs. Early exploratory studies of quasi-PDFs [24, 27–29] indeed suggested an asymmetric sea, even though renormalization was not yet available, and the computations were performed at large pion masses.

Recently, however, simulations at the physical pion mass, including a sophisticated treatment of renormalization, have shown a promising degree of agreement with empirical distributions [30, 31]. Nonetheless, a number of systematics, such as discretization and volume effects, as well as difficulties in dealing with high momentum hadrons on the lattice, have to be addressed before quantitative comparisons with phenomenology are possible. In this spirit, a measurement of the distribution $u - d$

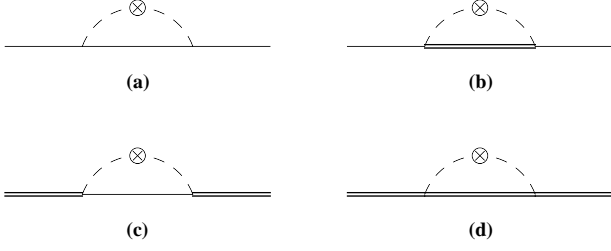


FIG. 1. Pion loop diagrams contributing to the $\bar{d} - \bar{u}$ PDFs in the nucleon (solid lines) and Δ (double solid lines) from the processes (a) $N \rightarrow N\pi$, (b) $N \rightarrow \Delta\pi$, (c) $\Delta \rightarrow N\pi$ and (d) $\Delta \rightarrow \Delta\pi$, with the \otimes representing the insertion of a nonlocal current operator.

in the Δ^+ would be of enormous interest, especially if the difference between the $u - d$ shapes in the Δ^+ and proton is sufficiently large compared to the present computational uncertainties.

Within a chiral effective theory framework, the asymmetry between the \bar{d} and \bar{u} PDFs in a baryon B ($B = N$ or Δ) arises through a convolution of the valence antiquark distribution in the pion, \bar{q}_v^π , and the corresponding light-cone momentum distribution, $f_{B \rightarrow B'\pi}$, of pions in B with a spectator baryon B' [14, 32–35]. The coupling of the external probe to the pion field in the effective theory arises through the rainbow diagrams illustrated in Fig. 1, as well as via bubble diagrams in which the pion loop couples to the baryon B via a Weinberg-Tomazawa four-point interaction [13, 14, 32–35]. The latter involve pions with zero momentum fractions y , and are localized to $x = 0$. Since lattice QCD simulations cannot access PDFs at $x = 0$, the bubble diagrams will not be relevant here.

Moreover, the rainbow diagrams themselves receive zero mode contributions [14, 34], in addition to the usual on-shell terms at $x > 0$. Off-shell and Kroll-Ruderman terms contribute to the quark distributions through coupling to the intermediate state baryon B' [32, 35]. In the following the distributions $f_{B \rightarrow B'\pi}$ (which are also referred to as chiral splitting functions) will denote only the on-shell components of the rainbow diagrams at $y > 0$. The dominant contributions to the antiquark asymmetry in the proton and Δ^+ are then given by

$$(\bar{d} - \bar{u})^p(x) = 2 \left[(f_{N \rightarrow N\pi} - f_{N \rightarrow \Delta\pi}) \otimes \bar{q}_v^\pi \right](x) \quad (1)$$

and

$$(\bar{d} - \bar{u})^{\Delta^+}(x) = \left[(f_{\Delta \rightarrow N\pi} + 2f_{\Delta \rightarrow \Delta\pi}) \otimes \bar{q}_v^\pi \right](x) \quad (2)$$

where the symbol “ \otimes ” denotes the convolution operator $[f \otimes g](x) \equiv \int_x^1 (dy/y) f(y) g(x/y)$.

For a proton target, the $N \rightarrow N\pi$ splitting function for Fig. 1(a) is given by the familiar expression [5, 34]

$$f_{N \rightarrow N\pi}(y) = \frac{g_A^2 M^2}{(4\pi f_\pi)^2} \int dk_\perp^2 \frac{y(k_\perp^2 + y^2 M^2)}{(1-y)^2 D_{NN}^2}, \quad (3)$$

where g_A is the nucleon axial charge, f_π is the pion decay constant, M is the nucleon mass, and k_\perp is the transverse momentum of the pion. The function D_{NN} is the pion virtuality $k^2 - m_\pi^2$, which in general depends on the initial and final state baryon masses, M_B and $M_{B'}$, respectively,

$$D_{BB'} = -\frac{k_\perp^2 - y(1-y)M_B^2 + yM_{B'}^2 + (1-y)m_\pi^2}{1-y}. \quad (4)$$

For the corresponding process $N \rightarrow \Delta\pi$ in Fig. 1(b), the splitting function is given by [33]

$$f_{N \rightarrow \Delta\pi}(y) = \frac{g_A^2}{25M_\Delta^2(4\pi f_\pi)^2} \int dk_\perp^2 \frac{y(\bar{M}^2 - m_\pi^2)}{1-y} \times \left[\frac{(\bar{M}^2 - m_\pi^2)(\Delta^2 - m_\pi^2)}{D_{N\Delta}^2} - \frac{\bar{M}^2 - 3m_\pi^2 + 2\Delta^2}{D_{N\Delta}} \right], \quad (5)$$

where M_Δ is the Δ mass, and we have defined $\bar{M} \equiv M + M_\Delta$ and $\Delta \equiv M_\Delta - M$. In the chiral limit, moments of the splitting functions can be expanded in power series in m_π , with the leading nonanalytic terms in the expansion, which depend only on the long-distance properties of pion loops, being model independent [36]. For the $N \rightarrow N\pi$ distribution one finds the characteristic leading order (LO) $\sim m_\pi^2 \log m_\pi^2$ nonanalytic behavior [10–14]. Moments of the $N \rightarrow \Delta\pi$ splitting function, in contrast, display the next-to-leading order (NLO) behavior $\sim m_\pi^4 \log m_\pi^2$ for $m_\pi \rightarrow 0$ [10, 13, 32, 33].

In the case of a Δ baryon initial state, the LO contribution is given by

$$f_{\Delta \rightarrow \Delta\pi}(y) = \frac{g_A^2}{50M_\Delta^2(4\pi f_\pi)^2} \int dk_\perp^2 \frac{y}{1-y} \times \left[\frac{m_\pi^2 [m_\pi^2(2M_\Delta^2 - m_\pi^2) - 10M_\Delta^4]}{D_{\Delta\Delta}^2} + \frac{m_\pi^2(4M_\Delta^2 - 3m_\pi^2) - 10M_\Delta^4}{D_{\Delta\Delta}} \right], \quad (6)$$

while the NLO distribution is

$$f_{\Delta \rightarrow N\pi}(y) = \frac{g_A^2}{50M_\Delta^2(4\pi f_\pi)^2} \int dk_\perp^2 \frac{y(\bar{M}^2 - m_\pi^2)}{(1-y)} \times \left[\frac{(\bar{M}^2 - m_\pi^2)(\Delta^2 - m_\pi^2)}{D_{\Delta N}^2} - \frac{\bar{M}^2 - 3m_\pi^2 + 2\Delta^2}{D_{\Delta N}} \right]. \quad (7)$$

In Eqs. (3)–(7) SU(6) symmetry and the Goldberger-Treiman relation have been used to write the πNN , $\pi N\Delta$ and $\pi\Delta\Delta$ couplings in terms of the common ratio g_A/f_π .

The splitting functions (3)–(7) are ultraviolet divergent and therefore need to be regularized. In the literature various regularization schemes have been advocated, including transverse momentum cutoff, Pauli-Villars and dimensional regularization (DR), as well as form factors or finite-range regulators [9, 32, 33, 35, 37]. The latter take into account the finite size of hadrons, while schemes

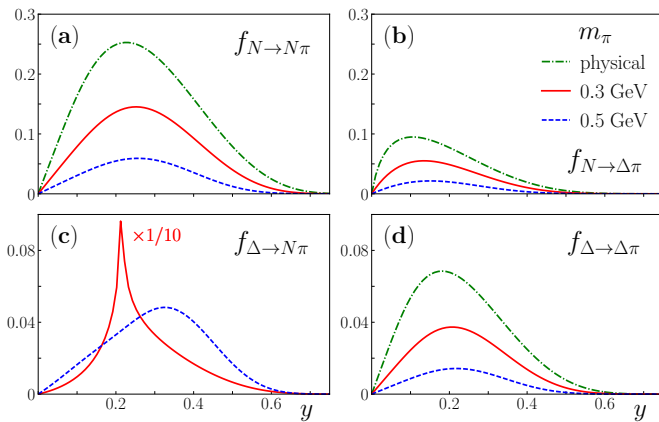


FIG. 2. Chiral splitting functions versus y for the (a) $N \rightarrow N\pi$, (b) $N \rightarrow \Delta\pi$, (c) $\Delta \rightarrow N\pi$ and (d) $\Delta \rightarrow \Delta\pi$ transitions at the physical pion mass (red solid curves), $m_\pi = 0.3$ GeV (blue dashed curves), and $m_\pi = 0.5$ GeV (green dot-dashed curves), using the exponential regulator with cutoff mass $\Lambda = 0.87$ GeV [40]. Note that the $\Delta \rightarrow N\pi$ function for $m_\pi = 0.3$ GeV is scaled by a factor $1/10$.

such as DR are generally more suitable for theories that treat hadrons as pointlike. The advantage of DR is that specific power counting schemes can be preserved in chiral perturbation theory expansions, whereas finite-range regulators effectively resum terms in the chiral series. In practice this allows for better convergence in m_π in regions where the usual power counting schemes would not otherwise be applicable [37, 38].

Following the phenomenological analyses [39, 40] of leading neutron deep-inelastic production data and other observables sensitive to chiral loops, we consider several forms for the regulator, including a k_\perp cutoff, k^2 -dependent exponential and monopole form factors, and a Regge theory motivated form [41]. In Fig. 2 we illustrate the four splitting functions (3)–(7) for a number of values of m_π relevant for lattice QCD simulations, for the case of the exponential form factor with cutoff mass $\Lambda = 0.87$ GeV. This value was obtained from the recent JAM global pion PDF analysis [40] including constraints on $\bar{d} - \bar{u}$ in the proton from pp and pd Drell-Yan data [16]. We take the same cutoff value for the $N\Delta\pi$ and $\Delta\Delta\pi$ couplings, and assume it to be independent of m_π (an assumption which is expected to break down at large m_π). The nucleon and Δ masses do have m_π dependence, on the other hand, and for these we take the approximate relations $M \approx M^{(0)} + m_\pi$ and $M_\Delta \approx M_\Delta^{(0)} + m_\pi$, with the chiral limit values $M^{(0)} = 0.8$ GeV and $M_\Delta^{(0)} = 1.1$ GeV [42].

For the case of the nucleon initial state, the dominance of the LO over the NLO contribution is obvious from Fig. 2(a) and (b). The reason is not only the smaller coupling but also the cost in energy to convert the nucleon into a Δ . On the other hand, for a Δ initial

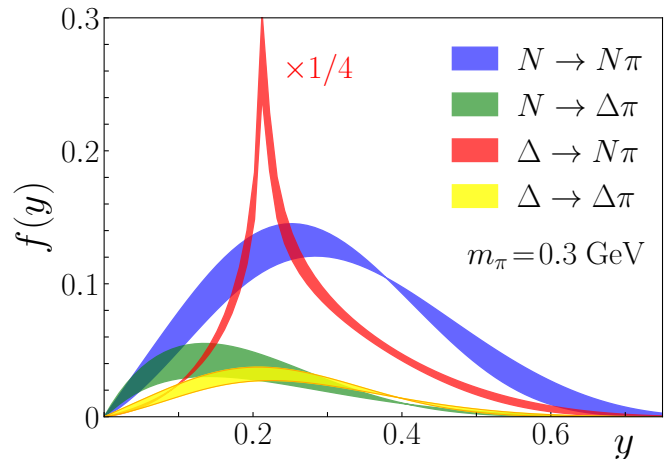


FIG. 3. Chiral splitting functions at $m_\pi = 0.3$ GeV, with the shaded bands representing the spread using the exponential and Regge form factor regulators [40]. Note that the $\Delta \rightarrow N\pi$ function is scaled by a factor $1/4$.

state the enhancement associated with the exothermic nature of the NLO $\Delta \rightarrow N\pi$ process means that it is larger than the LO $N \rightarrow N\pi$ contribution at all pion masses, and is also larger than the $N \rightarrow \Delta\pi$ function. At $m_\pi = 0.3$ GeV the most prominent feature in the $\Delta \rightarrow N\pi$ splitting function in Fig. 2(b) is the large cusp at $y \approx 0.2$, which indicates the opening of the octet decay channel at $m_\pi = \Delta$ (in the present analysis we take the mass difference $\Delta \approx 0.3$ GeV independent of m_π). Below this threshold the $\Delta \rightarrow N\pi$ function is complex, and is not shown in Fig. 2(c) at the physical pion mass. Compared to excited baryon masses, which are found to be relatively smooth functions of m_π across the pion decay threshold [37, 43], the additional pion propagator in the splitting function enhances the singularity at $m_\pi \approx \Delta$ to produce the observed spike. A similar behavior would also be expected for electroweak form factors, and indeed was observed in the calculation of pion loop corrections to the Δ magnetic moments [44].

To make a more direct comparison of the four processes, in Fig. 3 we compare the splitting functions at a fixed $m_\pi = 0.3$ GeV, at which the differences between the nucleon and Δ splitting functions are most dramatic. To explore the dependence of the results on the choice of regulator, we compare the results for the exponential form factor with those using the Regge form with cutoff $\Lambda = 1.43$ GeV, also from the JAM global PDF analysis [40]. The shaded bands in Fig. 3 represent the spread between the two calculations. As already indicated in Fig. 2, at this m_π value the $\Delta \rightarrow N\pi$ channel dominates, and the presence of the prominent cusp at $y \approx 0.2$ is independent of the choice of regulator. The contributions to the N and Δ splitting functions from the processes with $\Delta\pi$ intermediate states are significantly

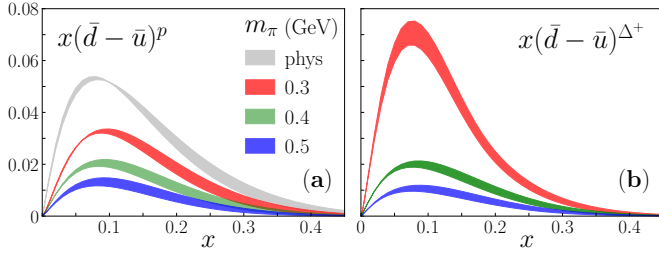


FIG. 4. Predicted x dependence of the $x(\bar{d} - \bar{u})$ asymmetry in (a) the proton and (b) Δ^+ baryon, for various pion masses: physical m_π (gray band), $m_\pi = 0.3$ GeV (red), 0.4 GeV (green), and 0.5 GeV (blue). The shaded bands represent the model dependence from the choice of regulator for the splitting function [40].

smaller than those for the $N\pi$ channels, regardless of the regulator form.

To obtain the x dependence of the $\bar{d} - \bar{u}$ distributions, the splitting functions in Figs. 2 and 3 need to be convoluted with the pion PDF. While pion valence PDF is relatively well determined from global next-to-leading-order analyses of Drell-Yan and other high energy scattering data [40, 45, 46], its dependence on m_π is less well understood. In the absence of direct lattice calculations of \bar{q}_v^π , Detmold *et al.* [48] used the several low PDF moments from lattice QCD simulations of pion twist-two matrix elements to reconstruct the x dependence over a range of pion masses from the chiral limit to $m_\pi = 1$ GeV, at a scale $Q^2 \sim 5$ GeV² set by the lattice spacing [47].

Using these inputs, in Fig. 4 we show the resulting $\bar{d} - \bar{u}$ asymmetry in the proton and Δ^+ for several m_π values ranging from the physical value (for the proton only) to $m_\pi = 0.5$ GeV. The bands in Fig. 4 represent uncertainties from the choice of ultraviolet regulator, corresponding to the spread in the splitting functions shown in Fig. 3. While the magnitude of the asymmetry in the proton and Δ^+ are similar for large values of $m_\pi \gtrsim 0.4$ GeV², the enhancement due to the opening of the decay channel at $m_\pi = \Delta$ renders the asymmetry in the Δ^+ twice as large near the peak in $x(\bar{d} - \bar{u})$ at $x \approx 0.1$.

The model dependence is expected to cancel to some extent in the ratio of the $\bar{d} - \bar{u}$ asymmetries in the Δ^+ and p , as illustrated in Fig. 5, where the lighter bands show the effect of the variation of the splitting functions in Fig. 3 for the different regulators. To highlight the strong enhancement of the Δ^+ asymmetry as one approaches the $N\pi$ threshold, we compute the ratio at $m_\pi = 0.3$ and 0.33 GeV (at which $(m_\pi - \Delta)/m_\pi \approx 10\%$), in addition to the 0.4 and 0.5 GeV values.

The variation with m_π is dramatic at $x \approx 0.1$, where the ratio goes from being $\approx 80\%$ at $m_\pi = 0.5$ GeV to $\gtrsim 200\%$ just above the threshold at $m_\pi = 0.3$ GeV. At larger x values, $x \gtrsim 0.25$, the ratios are close to unity for all the m_π values considered, albeit with larger uncer-

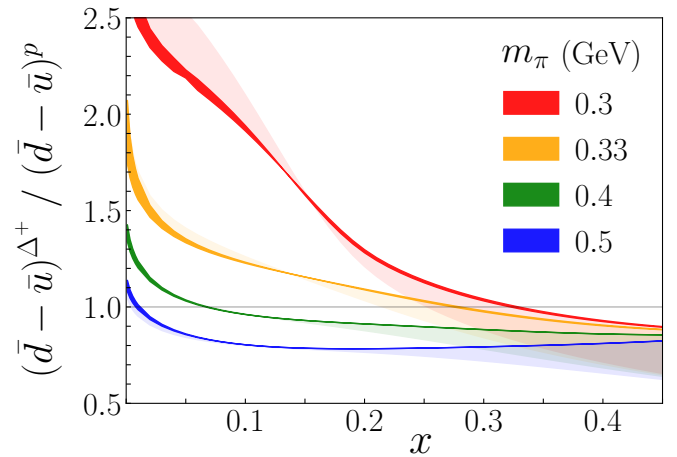


FIG. 5. Ratio of the $\bar{d} - \bar{u}$ asymmetry in the Δ^+ to that in the proton, for $m_\pi = 0.3$ (red), 0.33 (orange), 0.4 (green) and 0.5 GeV (blue bands). The darker bands represent the uncertainty on the pion PDF \bar{q}_v^π , while the lighter bands represent the dependence on the choice of regulator.

tainties. In this region the asymmetries are very small, however, and will in practice be difficult to extract from lattice or experiment.

The dependence of the asymmetry ratio on the input pion valence PDF is also relatively weak, as the darker bands in Fig. 5 illustrate. The bands represent the difference between the results using the splitting functions computed with the exponential regulator and the m_π dependent pion PDF from Ref. [48] with those using a fixed \bar{q}_v^π PDF at the physical pion mass. Since the same pion PDF enters both the Δ^+ and proton convolutions in the numerator and denominator for any m_π , the dependence on \bar{q}_v^π largely cancels, as expected.

The predicted large enhancement of the $\bar{d} - \bar{u}$ asymmetry in the Δ^+ can be tested in lattice QCD simulations at pion masses just above the $N\pi$ threshold where the Δ is stable. In particular, the ETM Collaboration plans to calculate the $u - d$ Δ quasi-PDF [49] using the Iwasaki improved gluon action and the twisted mass fermion action with clover improvement at several pion masses and lattice volumes [30]. These simulations should allow access to m_π values at which $(m_\pi - \Delta)/m_\pi \approx 3\%$ [24], which could provide a striking confirmation of the role of chiral symmetry and the pion cloud in the generation of a nonperturbative sea in baryons.

This work was supported by the University of Adelaide and by the Australian Research Council through the ARC Centre of Excellence for Particle Physics at the Terascale (CE110001104) and Discovery Project DP150103164, and the U.S. Department of Energy (DOE) Contract No. DE-AC05-06OR23177, under which Jefferson Science Associates, LLC operates Jefferson Lab.

-
- [1] P. Amaudruz *et al.*, Phys. Rev. Lett. **66**, 2712 (1991).
- [2] K. Gottfried, Phys. Rev. Lett. **18**, 1174 (1967).
- [3] A. W. Thomas, Adv. Nucl. Phys. **13**, 1 (1984).
- [4] S. Theberge, A. W. Thomas and G. A. Miller, Phys. Rev. D **22**, 2838 (1980) [Erratum: Phys. Rev. D **23**, 2106 (1981)].
- [5] A. W. Thomas, Phys. Lett. **126B**, 97 (1983).
- [6] W. Melnitchouk, A. W. Thomas and A. I. Signal, Z. Phys. A **340**, 85 (1991).
- [7] S. Kumano and J. T. Londergan, Phys. Rev. D **44**, 717 (1991).
- [8] E. M. Henley and G. A. Miller, Phys. Lett. B **251**, 453 (1990).
- [9] J. Speth and A. W. Thomas, Adv. Nucl. Phys. **24**, 83 (1997).
- [10] A. W. Thomas, W. Melnitchouk and F. M. Steffens, Phys. Rev. Lett. **85**, 2892 (2000).
- [11] W. Detmold, W. Melnitchouk, J. W. Negele, D. B. Renner and A. W. Thomas, Phys. Rev. Lett. **87**, 172001 (2001).
- [12] J. W. Chen and X. Ji, Phys. Lett. B **523**, 73 (2001).
- [13] D. Arndt and M. J. Savage, Nucl. Phys. **A697**, 429 (2002).
- [14] J. W. Chen and X. Ji, Phys. Rev. Lett. **88**, 052003 (2002).
- [15] A. Baldit *et al.*, Phys. Lett. B **332**, 244 (1994).
- [16] E. A. Hawker *et al.*, Phys. Rev. Lett. **80**, 3715 (1998).
- [17] W. Melnitchouk, J. Speth and A. W. Thomas, Phys. Rev. D **59**, 014033 (1998).
- [18] Fermilab E906 Experiment (SeaQuest), *Drell-Yan measurements of nucleon and nuclear structure with the Fermilab main injector*, <http://www.phy.anl.gov/mep/SeaQuest/index.html>.
- [19] X. Ji, Phys. Rev. Lett. **110**, 262002 (2013).
- [20] C. Alexandrou, K. Cichy, M. Constantinou, K. Hadjiyiannakou, K. Jansen, H. Panagopoulos and F. Steffens, Nucl. Phys. **B923**, 394 (2017).
- [21] J. W. Chen, T. Ishikawa, L. Jin, H.-W. Lin, Y. B. Yang, J. H. Zhang and Y. Zhao, Phys. Rev. D **97**, 014505 (2018).
- [22] J. Green, K. Jansen and F. Steffens, Phys. Rev. Lett. **121**, 022004 (2018).
- [23] X. Xiong, X. Ji, J. H. Zhang and Y. Zhao, Phys. Rev. D **90**, 014051 (2014).
- [24] C. Alexandrou, K. Cichy, V. Drach, E. Garcia-Ramos, K. Hadjiyiannakou, K. Jansen, F. Steffens and C. Wiese, Phys. Rev. D **92**, 014502 (2015).
- [25] T. Izubuchi, X. Ji, L. Jin, I. W. Stewart and Y. Zhao, arXiv:1801.03917 [hep-ph].
- [26] W. Detmold, W. Melnitchouk and A. W. Thomas, Mod. Phys. Lett. A **18**, 2681 (2003).
- [27] H.-W. Lin, J.-W. Chen, S. D. Cohen and X. Ji, Phys. Rev. D **91**, 054510 (2015).
- [28] J.-W. Chen, S. D. Cohen, X. Ji, H.-W. Lin and J.-H. Zhang, Nucl. Phys. **B911**, 246 (2016).
- [29] C. Alexandrou, K. Cichy, M. Constantinou, K. Hadjiyiannakou, K. Jansen, F. M. Steffens and C. Wiese, Phys. Rev. D **96**, 014513 (2017).
- [30] C. Alexandrou, K. Cichy, M. Constantinou, K. Jansen, A. Scapellato and F. Steffens, arXiv:1803.02685 [hep-lat].
- [31] J. W. Chen, L. Jin, H.-W. Lin, Y. S. Liu, Y. B. Yang, J. H. Zhang and Y. Zhao, arXiv:1803.04393 [hep-lat].
- [32] X. G. Wang, Chueng-Ryong Ji, W. Melnitchouk, Y. Salamu, A. W. Thomas and P. Wang, Phys. Rev. D **94**, 094035 (2016).
- [33] Y. Salamu, C. R. Ji, W. Melnitchouk and P. Wang, Phys. Rev. Lett. **114**, 122001 (2015).
- [34] M. Burkardt, K. S. Hendricks, C. R. Ji, W. Melnitchouk and A. W. Thomas, Phys. Rev. D **87**, 056009 (2013).
- [35] C. R. Ji, W. Melnitchouk and A. W. Thomas, Phys. Rev. D **88**, 076005 (2013).
- [36] A. W. Thomas and G. Krein, Phys. Lett. B **481**, 21 (2000).
- [37] R. D. Young, D. B. Leinweber and A. W. Thomas, Prog. Part. Nucl. Phys. **50**, 399 (2003).
- [38] J. M. M. Hall, D. B. Leinweber and R. D. Young, Phys. Rev. D **82**, 034010 (2010).
- [39] J. R. McKenney, N. Sato, W. Melnitchouk and C.-R. Ji, Phys. Rev. D **93**, 054011 (2016).
- [40] P. C. Barry, N. Sato, W. Melnitchouk and Chueng-Ryong Ji, Phys. Rev. Lett. **121**, xxxxx (2018).
- [41] B. Z. Kopeliovich, I. K. Potashnikova, B. Povh and I. Schmidt, Phys. Rev. D **85**, 114025 (2012).
- [42] A. Walker-Loud, PoS LATTICE **2008**, 005 (2008) [arXiv:0810.0663 [hep-lat]].
- [43] D. B. Leinweber, A. W. Thomas, K. Tsushima and S. V. Wright, Phys. Rev. D **61**, 074502 (2000).
- [44] I. C. Cloet, D. B. Leinweber and A. W. Thomas, Phys. Lett. B **563**, 157 (2003).
- [45] P. J. Sutton, A. D. Martin, W. J. Stirling, R. G. Roberts, Phys. Rev. D **45**, 2349 (1992).
- [46] M. Aicher, A. Schäfer and W. Vogelsang, Phys. Rev. Lett. **105**, 252003 (2010).
- [47] C. Best *et al.*, Phys. Rev. D **56**, 2743 (1997).
- [48] W. Detmold, W. Melnitchouk and A. W. Thomas, Phys. Rev. D **68**, 034025 (2003).
- [49] F. M. Steffens, C. Alexandrou, S. Bacchio, K. Cichy *et al.*, Δ -baryon parton distribution functions from lattice QCD, Project Proposal for Tier 0/Tier 1 HPC Access, Gauss Centre for Supercomputing.